AN INVESTIGATION OF THE PERFORMANCE OF AN INDUCTION TYPE MOTOR WITH METAL INCLOSED STATOR

BY

L. H. RATHBUN, JR.

AN INVESTIGATION OF THE PERFORMANCE OF AN INDUCTION TYPE MOTOR WITH METAL INCLOSED STATOR

-

L. H. Rathbun, Jr.

AN INVESTIGATION OF THE PERFORMANCE OF AN INDUCTION TYPE MOTOR WITH METAL INCLOSED STATOR

by

Leon Herbert Rathbun, Jr.
Lieutenant Commander, United States Navy

Submitted in partial fulfillment
of the requirements
for the degree of
MASTER OF SCIENCE
in
Electrical Engineering

United States Naval Postgraduate School
Annapolis, Maryland
1951

This work is accepted as fulfilling

the thesis requirements for the degree of

MASTER OF SCIENCE
in
Electrical Engineering

from the

United States Naval Postgraduate School.

PREFACE

This thesis subject was suggested by Dr. J. B. Friauf of the Navy Department, Bureau of Ships. It was desired to determine the practicability of a motor designed with a sealed stator and an open free flooding rotor for use under water; and also to develop the theory of this "canned stator" motor.

An ordinary wound rotor induction motor was used with the rotor shorted to obtain the characteristics of a squirrel cage motor. It was originally thought that the rotor would have to be turned down in order to permit insertion of the metal cylinder into the air gap. However, air gap clearances were sufficient to permit insertion of the cylinder without modifying the motor.

It is wished to acknowledge the assistance given by Dr. Friauf of the Bureau of Ships and by Professor C. V. O. Terwilliger of the Postgraduate School in conducting this investigation.

This work was performed between August 1950 and May 1951 at the U.S. Naval Postgraduate School, Annapolis, Maryland.

TABLE OF CONTENTS

TABLE OF SYMBOLS

β_m	maximum value of field flux
b_e	primary exciting susceptance
C	circumferential length of metal cylinder
E_s	voltage generated in axial strip of cylinder
E_2	secondary voltage to neutral at standstill
g_e	primary exciting conductance per phase, representing core loss and friction and windage current
I_1	primary current per terminal
I_e	primary exciting current per terminal
I_L	power loss component of exciting current
I_{2s}	secondary current per phase at slip s
I_m	magnetizing current per phase
l	axial length of metal cylinder
N_s	number of axial strips in cylinder
P_s	power loss per strip
P_c	power loss in cylinder
R_o	total equivalent resistance
R_1	primary resistance
R_2	secondary equivalent resistance
R	equivalent load resistance
s	slip in per unit values
t	thickness of cylinder
v	peripheral velocity of stator field
V	impressed voltage
X_o	total equivalent leakage reactance

X_1 primary leakage reactance per phase

X_2 secondary leakage reactance per phase at standstill

X_{2s} secondary leakage reactance per phase at slip s

X_0 total equivalent leakage reactance

Z_0 total equivalent impedance

ρ resistivity of cylinder

θ_{2s} angle of lag between V and I_{2s}

LIST OF ILLUSTRATIONS

CHAPTER I

OBJECTIVES

The "canned stator" induction motor would consist of a squirrel cage induction motor with the stator completely inclosed by a thin metal sheet, but with the rotor uninclosed. Part of the stator seal would lie in the air gap in the form of a metal cylinder fixed to the stator, and completely shielding the rotor from the stator. The purpose of this arrangement is to make the motor suitable for use under water.

The object of this study is to determine the effect of such a metal cylinder in the air gap on the performance of the machine, and also to compare the effect of varying the type of metal used. The operating characteristics of the motor are considered to be affected only by that portion of the stator seal which lies within the air gap; inasmuch as all but a negligible amount of working flux cutting the rotor passes through the air gap. Consequently, it was unnecessary as well as impracticable to completely enclose the stator in order to accomplish the investigation. Instead, a thin metal cylinder was placed in the air gap and firmly fixed against the stator. A slight overhang of approximately three fourths of an inch was allowed at each end of the cylinder. Experimental data was obtained from this arrangement.

The ultimate design of the motor under study would consist of a hermetically sealed stator with suitable water

tight and pressure proof bushings for electrical connections, and an unenclosed, free flooding rotor connected to the load. Such a motor would be used to drive certain machinery aboard ship of a vital nature, and in such location that it might be flooded in the event of collision or battle damage. As a submersible motor its advantages are: (a) no difficulty exists in providing adequate water tight seals around a rotating shaft, since only the stationary part of the motor is enclosed; (b) cooling problems would be less in non-submerged operation compared to a fully enclosed submersible motor. On the other hand, disadvantages of the enclosed stator motor would include (a) increased cost and difficulty of manufacture; (b) additional windage losses when the motor is operating submerged.

CHAPTER II

LOSSES IN THE METAL CYLINDER

The effect of the metal cylinder in the air gap is to cause losses in addition to the normal losses of the unmodified induction motor. Practically all of the stator field flux crossing the air gap and cutting the rotor conductors will also cut the cylinder; especially since the cylinder extends beyond the ends of the rotor. As the stator field flux revolves at synchronous speed it will induce voltages in the cylinder which in turn will cause eddy currents to flow.

To determine the approximate distribution of these eddy currents, the cylinder may be thought of as a blocked squirrel cage rotor. The rotor bars consist of a large number of small axial strips an infinitesimal distance apart, shorted by end rings. The overhanging ends of the cylinder are considered the end rings. The space distribution of the stator flux is generally sinusoidal. The instantaneous voltages introduced in the axial strips are directly proportional to the flux density at the respective strip at any one instant. Since the flux is sinusoidal in distribution, the space envelope of the instantaneous voltages is also a sine wave. These voltages and flux waves are shown in Figure 1.

These eddy currents existing in the metal cylinder constitute additional losses in the induction motor over and above the losses existing in an ordinary machine. The

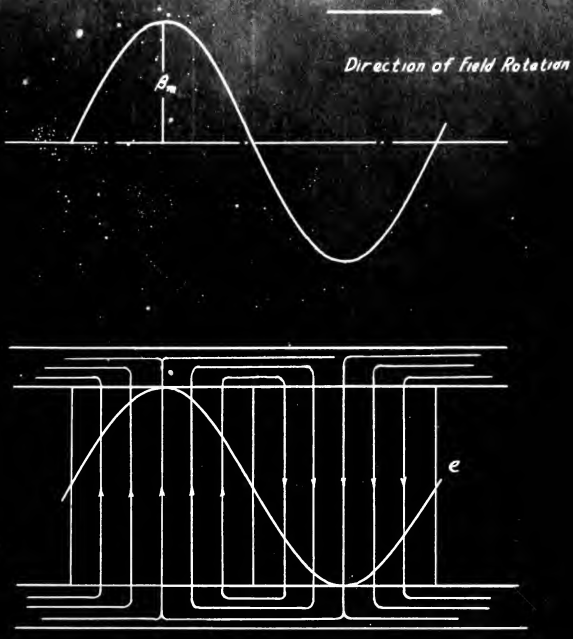

Field Flux and Voltages Induced in Cylinder
FIGURE 1

losses in the latter are friction and windage, primary and secondary core loss, primary and secondary copper loss, and stray load loss. Since the cylinder is essentially a fixed part of the stator, subject to the same frequency as the stator, the cylinder losses are of the same nature as that component of primary core loss caused by eddy currents alone. There are no hysteresis losses in the cylinder since the metals used were non-magnetic, or nearly so.

In analyzing the losses due to these voltages and the eddy currents resulting, assume a sinusoidal space distribution of flux moving at synchronous speed around the stator. The voltage induced in any one bar, or axial strip, is:

$$E_s = B l v \times 10^{-8} \tag{1}$$

where $B = \frac{2}{\pi} B_m$

l the active length of the strip

v the peripheral speed of the stator field

The current in the strip causing power loss is E_s / r_s, and the power loss due to these eddy currents is E_s^2 / r_s where r_s is the resistance of the individual strip. To find the power loss in terms of cylinder constants:

N_s the number of strips in the cylinder (arbitrary)

C the circumferential length of the cylinder

t the thickness of the cylinder

ρ the resistivity of the cylinder metal

Then

$$r_s = \rho \frac{l}{A} = \rho \frac{l}{tC/N_s} \tag{2}$$

The power loss per strip, P_s is

$$P_s = \frac{E_s^2}{r_s} = \frac{E_s^2 Ct}{\rho l N_s} \tag{3}$$

The total power loss for the cylinder, P_c is

$$P_c = N_s P_s = \frac{E_s^2 Ct}{\rho l} \tag{4}$$

Substituting from (1)

$$P_c = \frac{(B l v \cdot 10^{-8})^2 Ct}{\rho l} = \frac{KB^2 t}{\rho} \tag{5}$$

From this it appears that insofar as the cylinder is concerned, the additional losses will vary inversely as the resistivity of the cylinder and directly as the thickness. Actually, the approximations involved in attempting to analyze the losses render Equation (5) of qualitative value mainly. No design data was available for the motor to determine the field flux quantitatively. Also the distribution of eddy currents is not predictable, since the axial strips are not separated, and the eddy currents undoubtedly circulate more at random in the motor than indicated by Figure 1. A comparison of actual measured cylinder losses for different types of metal is made later.

CHAPTER III

EXPERIMENTAL PROCEDURE AND RESULTS

1. Description of Test Arrangement

As previously noted, the investigation was concerned only with the effect of the metal cylinder in the air gap on the performance of the motor. The motor used was a 5 kva, 220 volt, three phase wound rotor induction motor. Since only a squirrel cage motor could be used in actual operation, the rotor was shorted in all the tests in order to obtain squirrel cage characteristics. Running light tests and blocked rotor tests were run for each of four conditions as follows:

a. Motor unmodified

b. Non-magnetic steel cylinder inserted in the air gap

c. Brass cylinder inserted in the air gap

d. Copper cylinder inserted in the air gap

The bearings were adjusted to give a uniform air gap dimension of .0225 inches. In order to insert each cylinder, the rotor was removed. The cylinder was then fitted firmly into position around the inside of the stator, and the motor reassembled. The metallic cylinders had thicknesses as follows:

Steel	.0095 inches
Brass	.010 inches
Copper	.011 inches

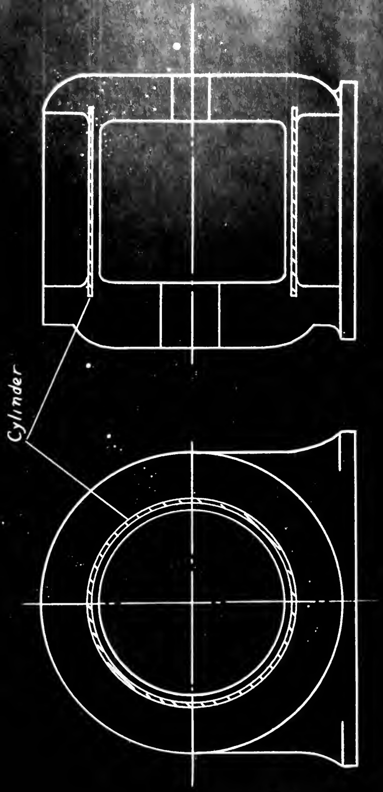

Sketch of Cylinder Arrangement in Motor

FIGURE 2.

The metal cylinder took up almost one half of the available air gap, and careful reassembly of the motor was necessary in order to prevent any rubbing. This was accomplished satisfactorily. Figure 2 shows a sketch of the modified motor with the cylinder in place.

2. The Equivalent Circuit

It was decided to use the equivalent circuit and the circle diagram as the basis for comparison of the unmodified motor and the motor with various types of cylinders in the air gap. The i^2r losses existing in the metal cylinder are of the same nature as eddy current losses in the stator, and they are treated as additional core losses in the determination of the parameters of the equivalent circuit, and in obtaining the circle diagram.

The equivalent circuit for the induction motor is shown in Figure 3 (a) for the rotor at standstill. The motor is then a transformer with the secondary shorted, and f_1 is equal to f_2. When the secondary rotates, the secondary frequency changes to sf_2, and the voltage generated per turn is no longer the same for the two coils. Figure 3 (b) shows this condition. To further simplify the circuit:

$$X_{2s} = sX_2 \tag{1}$$

$$\dot{E}_{2s} = s\dot{E}_2 = \dot{I}_{2s}(R_2 + jsX_2) \tag{2}$$

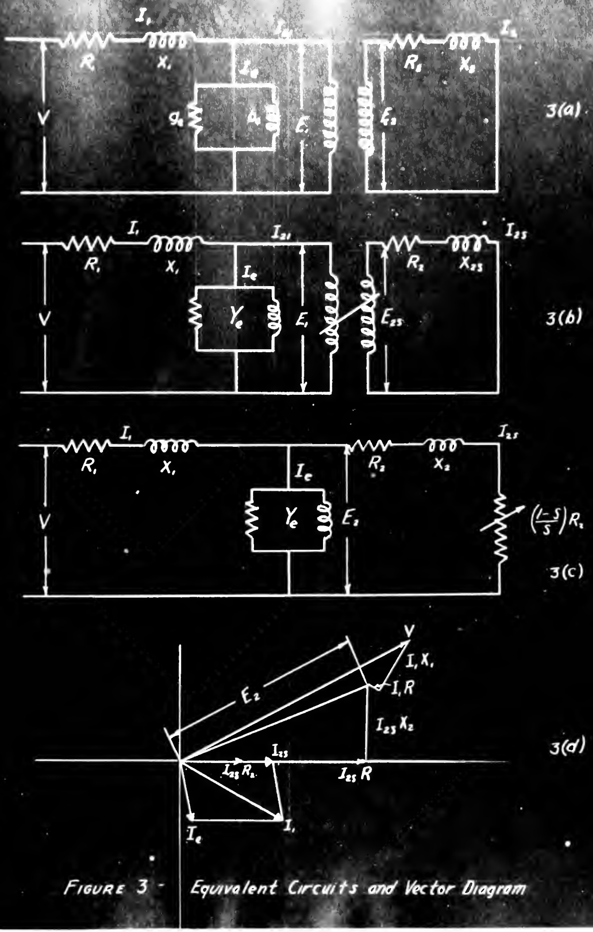

FIGURE 3 - Equivalent Circuits and Vector Diagram

Therefore

$$\dot{I}_{2s} = \frac{s\dot{E}_2}{R_2 + jsX_2} \qquad (3)$$

Dividing numerator and denominator by s we get

$$\dot{I}_{2s} = \frac{\dot{E}_2}{R_2/s + jX_2} \qquad (4)$$

Since

$$\frac{R_2}{s} = R_2 + \frac{(1-s)}{s} R_2 \qquad (5)$$

The expression $\frac{(1-s)}{s} R_2$ now represents the electrical equivalent of the load. Furthermore, if the values in the secondary are converted to equivalent primary values in accordance with the turns ratio, the equivalent circuit diagram becomes that of Figure 3 (c). The vector diagram is shown in Figure 3 (d).

If the circuit parameters are known, all equations expressing the currents and voltages in terms of these parameters and the impressed voltage may be derived from Figure 3 (c).

3. Tests on the Unmodified Motor.

To determine the motor constants and the circle diagram, standard running light tests and blocked rotor tests were made. Stator and rotor resistances were measured by a Kelvin bridge, and the stator - rotor turns ratio also measured.

We will discuss the results obtained for the unmodified motor first, and then compare with the motor performance with metal cylinders installed. In the running light test readings were taken of impressed voltage, primary current, primary power input, and speed. These data are shown in Appendix 2. No readings were used for more than 8 per cent slip. The data was plotted as shown in Figure 4. By extrapolating the power curve to the point of zero voltage, where flux density and hence core loss are zero, we can determine the friction and windage loss. This loss is shown by the horizontal straight line, and is nearly constant, since the speed was nearly constant. The $I_1^2 R_1$ loss is also plotted as shown, and the net loss after subtracting these two losses is the primary core loss. The secondary core loss and copper loss are negligible, since both the slip and the load are quite small. The equivalent circuit diagram for the running light test is shown in Figure 5 (a). An approximation has been made, in that the voltage drop of the exciting current through the primary impedance is neglected, i.e. the exciting path has been moved to the impressed voltage side of the primary impedance. The error is relatively small, and is acceptable for the purpose of simplifying calculations. The vector diagram for this circuit is shown in Figure 5 (b). If the sum of the friction and windage losses and the secondary core losses are assumed approximately constant over the operating range of the motor, then the component of secondary current corresponding to these losses may also be transferred to the exciting path. Figure

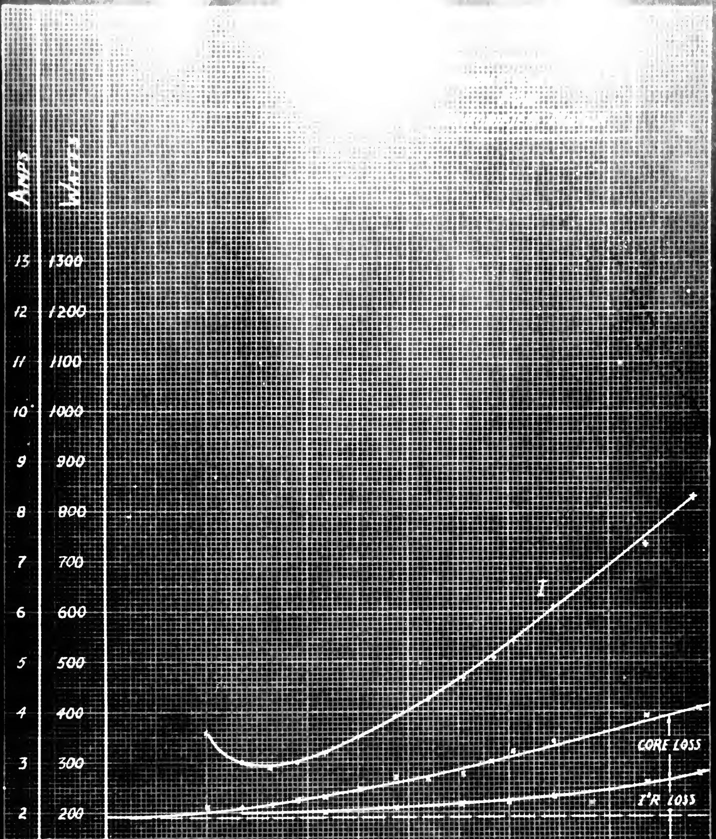
AMPS
WATTS
13
1300
12
1200
11
1100
10
1000
9
900
8
800
7
700
6
600
5
500
4
400
3
300
2
200
1
100
0
0
20
40
60
80
100
120
140
160
180
200
220
VOLTS
I
CORE LOSS
I²R LOSS
FRICTION + WINDAGE

FIGURE 4.

5(a)

Equivalent Circuit - Running Light Test

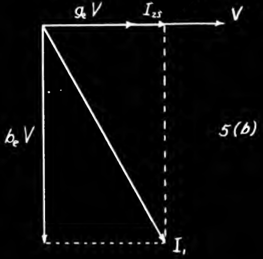

5(b)

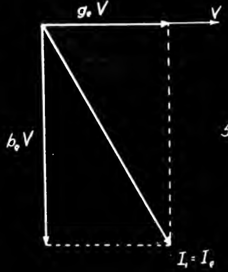

5(c)

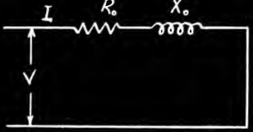

5(d)

Equivalent Circuit - Blocked Rotor Test

FIGURE 5.

5 (b) is then reduced to Figure 5 (c).

The following results may then be obtained on a per phase basis:

$$I_e = I_1 \tag{6}$$

$$I_l = \frac{P}{V\sqrt{3}} \tag{7}$$

$$I_m = \sqrt{I_1^{\,2} - I_l^{\,2}} \tag{8}$$

$$g_e = \frac{I_l\sqrt{3}}{V} \tag{9}$$

$$b_e = \frac{I_m\sqrt{3}}{V} \tag{10}$$

Numerical values for the above for each test condition of the motor are tabulated in Appendix 5 for comparison.

The blocked rotor test is usually made at reduced voltage V_b ; therefore, the blocked rotor current I_b is relatively small, and the saturation of the iron in the paths of the leakage flux is not noticeable. If the locked current is then determined for rated voltage, V, by multiplying I_b by the ratio V/V_b the value resulting is smaller than the actual blocked rotor current at full voltage. Due to saturation of the leakage paths at high currents, the locked current is appreciably higher than it would be without saturation; i.e., the equivalent

leakage reactance is not constant, but decreases as saturation becomes appreciable.

The influence of saturation in the leakage paths occurs only at high current and high slip. Since there is no saturation at normal currents, we use the non-saturated leakage reactance to determine the performance of the motor at small slip. If this limitation is kept in mind, the equivalent circuit and circle diagram provide an adequate basis of comparison between the unmodified motor and the "canned stator" motor over the normal operating range of the motor. This is confined to about the first third of the circle nearest the running light point.

The results of the blocked rotor test are shown in Figure 6. The voltage drop is due almost entirely to the short circuit currents flowing through their respective impedances. The core loss is very small because of the greatly reduced flux, and can be neglected. The equivalent circuit is shown in Figure 5 (d); and the power readings are attributed entirely to the I^2R losses in the primary and secondary.

The following results are then obtained on a per phase basis:

$$Z_o = \frac{V_b}{I_b \sqrt{3}} \qquad (11)$$

$$R_o = \frac{P_b}{3 I_b^2} \qquad (12)$$

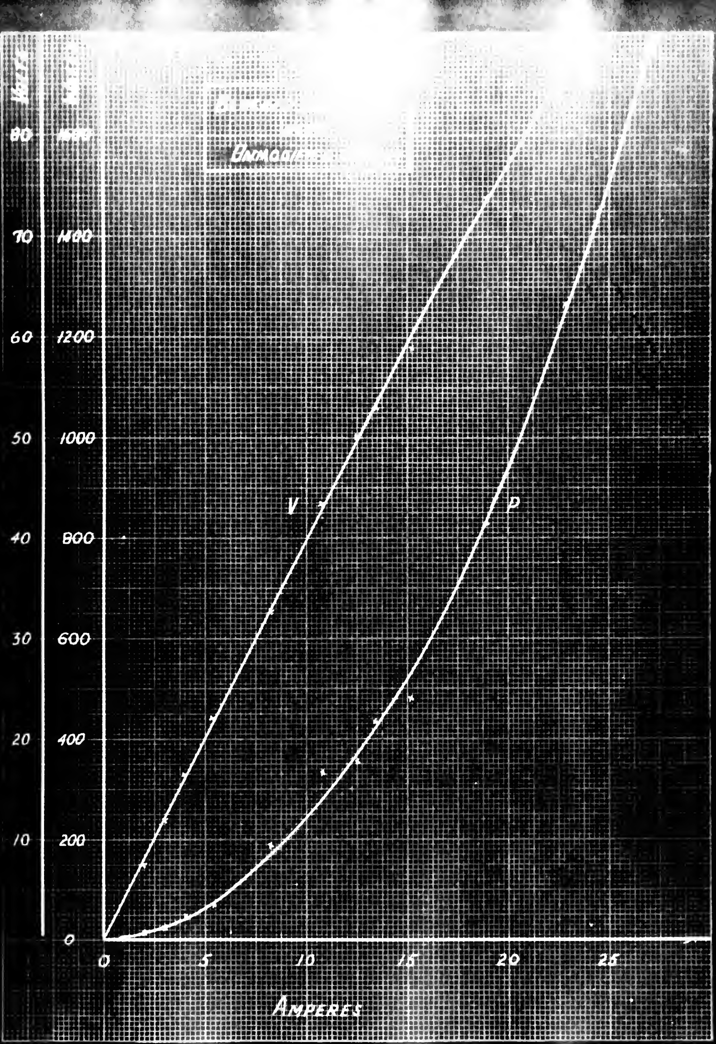
80
70
60
50
40
30
20
10
1400
1200
1000
800
600
400
200
0
V
P
0
5
10
15
20
25
AMPERES

FIGURE 6

(11)

(12)

The measured values of the primary resistance R_1 and the secondary resistance R_2 corrected for temperature added together should be equal to R_0. R_2 must be converted to the equivalent primary resistance, of course.

$$X_0 = \sqrt{Z_0^2 - R_0^2} \tag{13}$$

It is assumed that

$$X_1 = X_2 = X_0/2$$

Numerical values for the above are also tabulated in Appendix 5.

The approximate circle diagram is developed as follows. The equivalent circuit is shown in Figure 5 (a). The equivalent load resistance $R = \frac{(1-S)}{S} R_2$

Then
$$I_{2S} = \frac{V}{\sqrt{(R_1 + R_2 + R)^2 + (X_1 + X_2)^2}} \tag{14}$$

I_{2S} lags V by an angle θ_{2S} such that

$$\sin \theta_{2S} = \frac{X_1 + X_2}{\sqrt{(R_1 + R_2 + R)^2 + (X_1 + X_2)^2}} \tag{15}$$

Therefore
$$I_{2S} = \frac{V \sin \theta_{2S}}{X_1 + X_2} \tag{16}$$

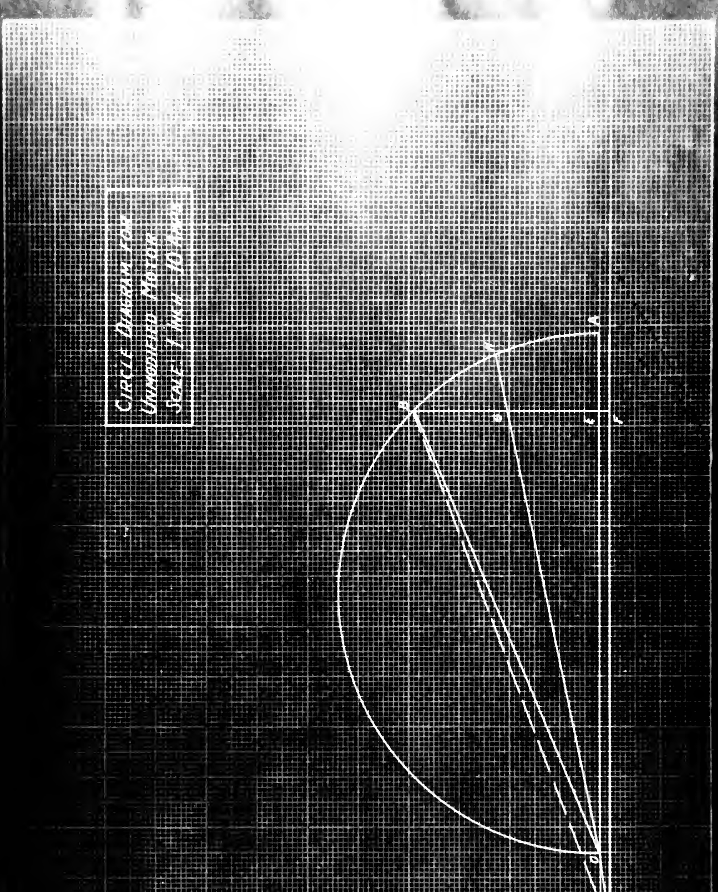

FIGURE 7

This is the polar equation of a circle, assuming X_1 and X_2 to be constant. Also, the primary current is

$$\dot{I}_1 = \dot{I}_{2s} + \dot{I}_e \tag{17}$$

where I_e is the no load current.

The combined circle diagram for the unmodified motor is shown in Figure 7. It is constructed for the data obtained in the no load and blocked rotor tests. Computations and results are shown in Appendix 6.

4. Tests on the Motor with Steel Cylinder in Air Gap

The motor with the non-magnetic steel cylinder installed was given the same tests as described in Section 3. The no load tests show appreciably higher core losses than for the unmodified motor. These results are shown in Figure 8. The unmodified motor had core losses of 125 watts at rated voltage. The core losses with the steel cylinder were 500 watts. The running light current was only slightly higher for the steel cylinder modification. This increase in running light current was due to the increased power loss component, and the magnetizing current remained practically unchanged. The friction and windage losses were also unchanged.

Determination of the equivalent circuit parameters, and the approximate circle diagram proceeded as in Section 3. The computations are shown in Appendix 5. One modification was made, however. In the blocked rotor test the core losses are neglected because the main flux is greatly reduced.

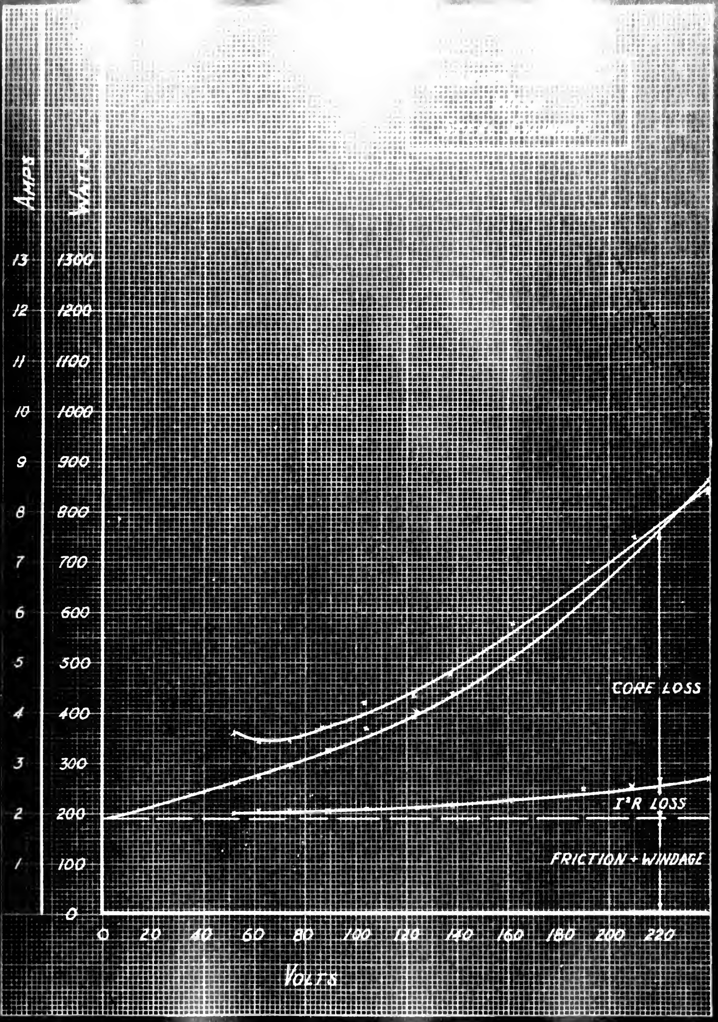
AMPS
WATTS
13
12
11
10
9
8
7
6
5
4
3
2
1
1300
1200
1100
1000
900
800
700
600
500
400
300
200
100
0
CORE LOSS
I²R LOSS
FRICTION + WINDAGE
0
20
40
60
80
100
120
140
160
180
200
220
VOLTS

FIGURE 8

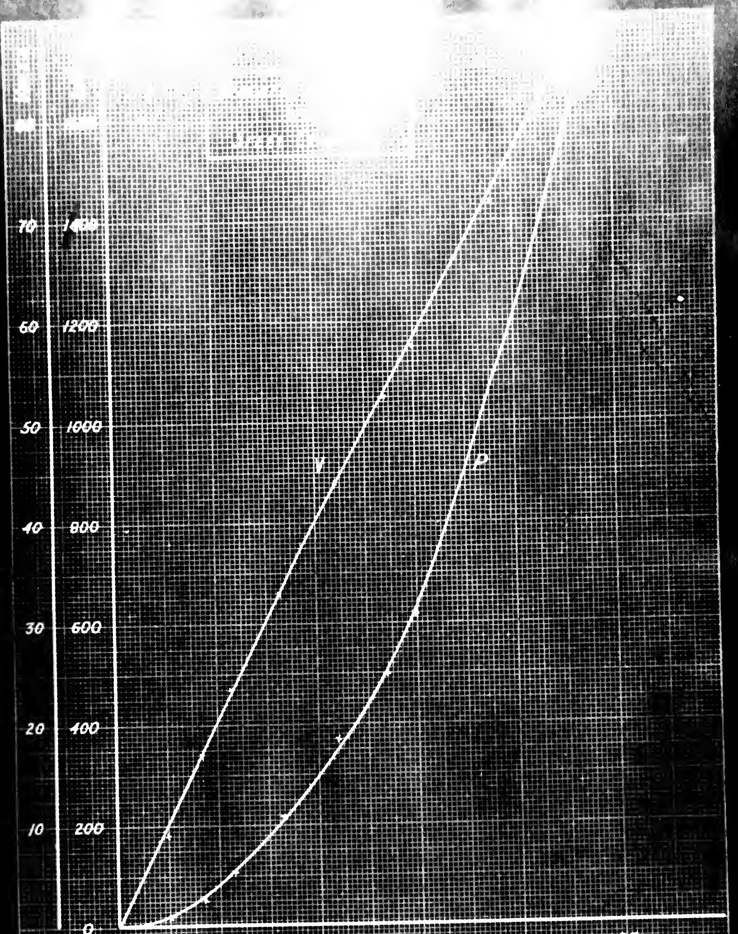

70
1400
60
1200
50
1000
40
800
30
600
20
400
10
200
0
V
P
0
5
10
15
20
25
AMPERES

FIGURE 9

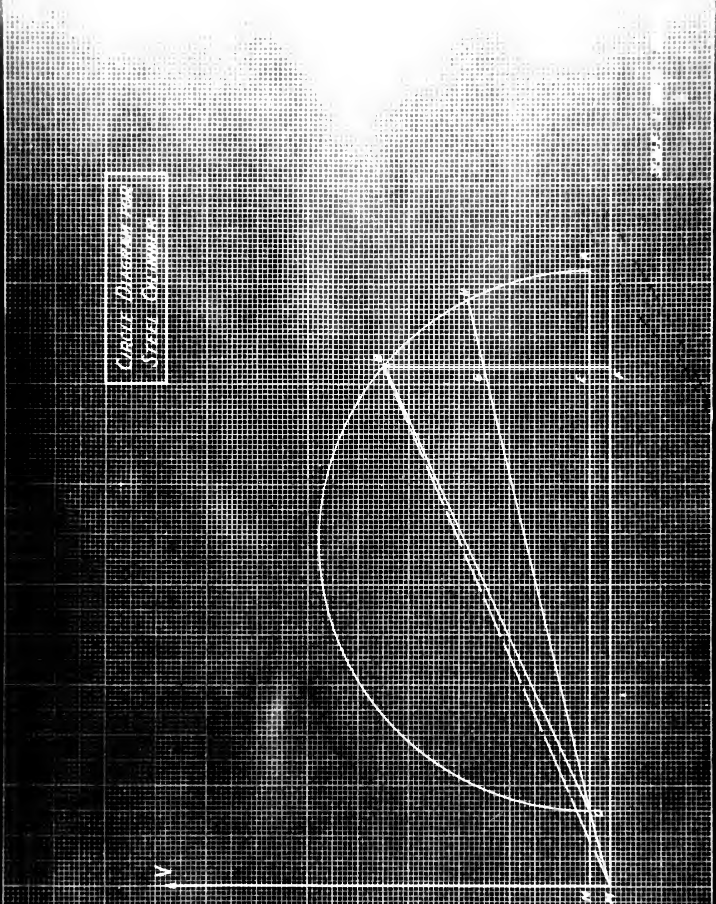

FIGURE 10

However, power readings for this test with the cylinder inserted are higher than for the unmodified motor. This additional loss is due to the cylinder, since R_1 and R_2 are unchanged. This additional loss is plotted in Figure 13. The correct value for the test voltage is obtained from Figure 13, and subtracted from the blocked rotor power reading to yield the actual copper loss. The results of the blocked rotor test are shown in Figure 9, and the circle diagram in Figure 10.

5. Tests on the Motor with Brass Cylinder in Air Gap

With the brass cylinder installed, similar tests were run as described previously. The core losses increased sharply over those of the steel cylinder. They amounted to 1170 watts at rated voltage. This is shown in Figure 11. A comparison of the core losses versus impressed voltage for the three conditions of the motor is shown in Figure 12. The losses increase with the conductivity of the cylinder as expected, but are not directly proportional. The measured resistivity of the steel was 465 ohms/ circular mil foot, compared to 44.05 ohms/circular mil foot for the brass. Although the conductance of the brass is more than ten times that of the steel, the losses are only a little more than double.

The no load current also increased very sharply. It measured 13 amperes, equivalent to the rated load current of the unmodified machine. The increase was caused mainly by the increase in I_m rather than by the additional power

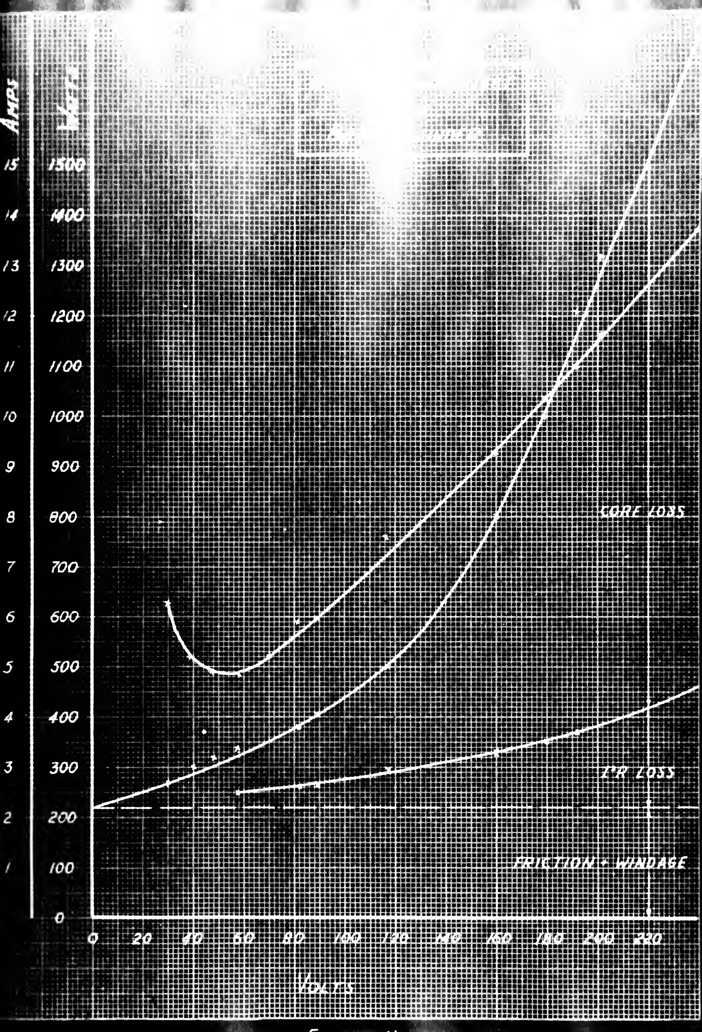

AMPS
WATTS
15
1500
14
1400
13
1300
12
1200
11
1100
10
1000
9
900
8
800
7
700
6
600
5
500
4
400
3
300
2
200
1
100
0
0
20
40
60
80
100
120
140
160
180
200
220
VOLTS
CORE LOSS
I²R LOSS
FRICTION + WINDAGE

FIGURE 11.

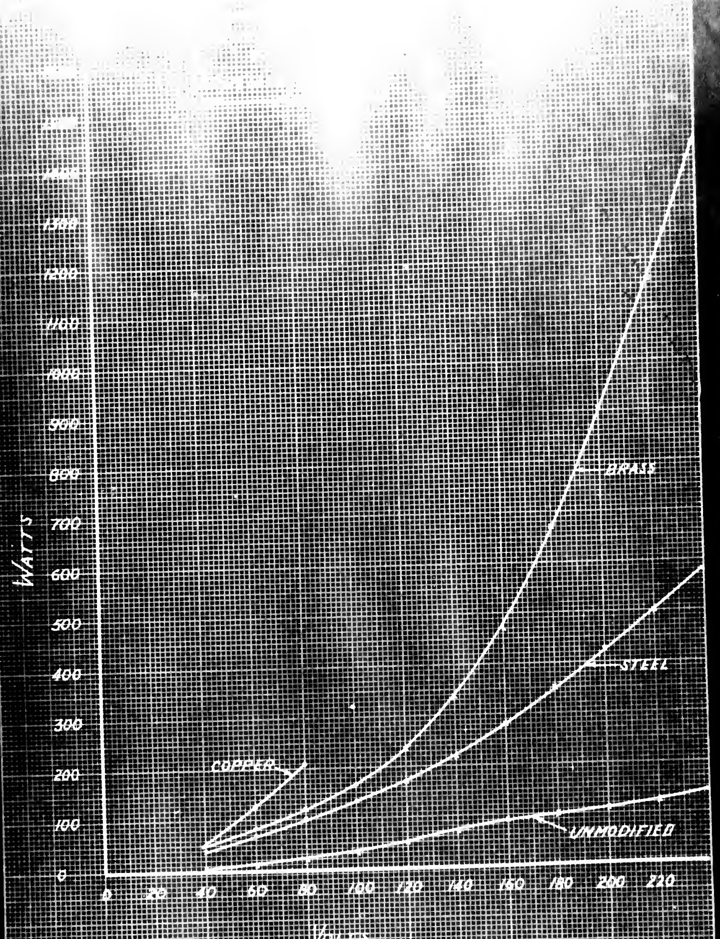
WATTS
1300
1200
1100
1000
900
800
700
600
500
400
300
200
100
0
0
20
40
60
80
100
120
140
160
180
200
220
VOLTS
BRASS
STEEL
COPPER
UNMODIFIED

FIGURE 12

component of the no load current. For the unmodified motor, and the motor with the steel cylinder, I_m was 7.54 amperes. With the brass can installed, I_m increased to 12.3 amperes. Apparently, with the introduction of low resistance material in the can, the eddy currents are no longer quite analogous to core losses. Instead, the can acts like a permanently installed blocked rotor. This effect acts to decrease the main flux, and requires a great deal more exciting current. It would also account for the fact that additional eddy current losses in the can are lower than expected; for although resistivity has decreased, β , the flux density has also decreased.

The standard circle diagram analysis may not be of much value for the motor with a low resistance cylinder. However, computations were made on the basis of test results, and are shown in Appendix 5. The blocked rotor test results are shown in Figure 13 and the circle diagram in Figure 14. The analysis of this type motor is not essential to the purpose of the investigation, because the motor has extremely high additional losses, and draws almost full rated current at no load. For these reasons it is unsuitable for the use desired.

6. Tests on the Motor with Copper Cylinder in Air Gap

The final tests were made with a copper cylinder installed in the air gap. The measured resistivity of the copper was 11.15 ohms/circular mil foot. We would expect that motor operation in this case would result in prohibitive losses, and a large no load current. When 212

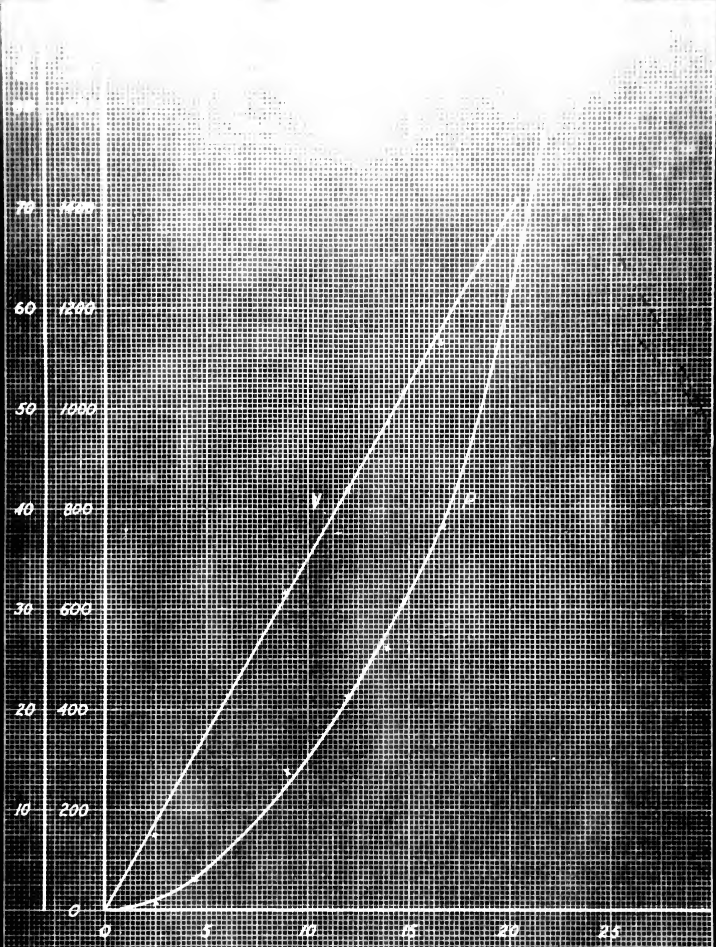
70
60
50
40
30
20
10
1400
1200
1000
800
600
400
200
0
V
0
5
10
15
20
25
AMPERES

FIGURE 13.

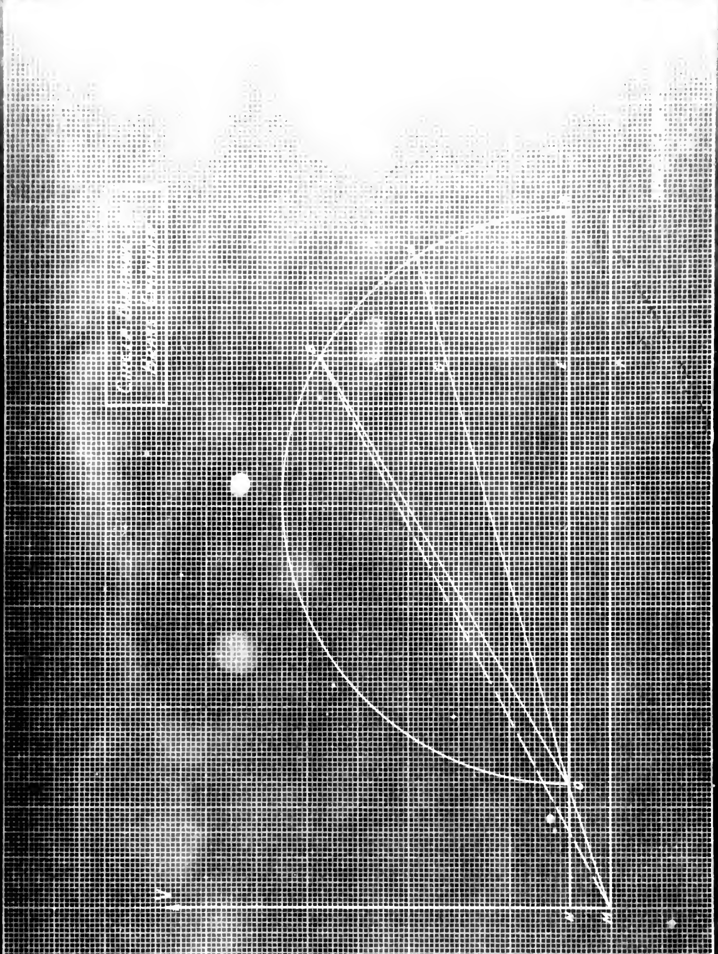

FIGURE 14.

volts were impressed on the motor for a no load test, the current read approximately 50 amperes, or 300 per cent over normal load current. No current and power data were taken under these conditions, particularly since the motor windings began to smoke almost immediately. It was also impossible to make a satisfactory test at lower voltages, because the motor refused to turn at more than 140 rpm, even with 200 per cent full load current in the primary.

Consequently, no analysis has been attempted for this motor. From a practical standpoint, the motor with copper cylinder installed is virtually useless, as it draws prohibitive current, with large losses, and hence has extremely low efficiency.

CHAPTER IV

CONCLUSIONS

From the circle diagrams, Figures 1, 10, and 14, comparative curves for efficiency, power factor, speed, and primary current versus torque were plotted. These curves are shown in Figures 15 and 16. The curves were not extended to the point of starting torque for reasons previously discussed. These curves indicate that the motor with the steel cylinder has slightly inferior performance to the unmodified motor, and the performance with the brass cylinder installed is inferior to both. The characteristics of the enclosed stator motor can be made to approach those of the unmodified motor by increasing the resistance of the cylinder by:

1. Decreasing the thickness of the cylinder
2. Increasing the resistivity of the cylinder

The first method has limited application. The cylinders used were almost a minimum in thickness for adequate strength and suitability for ordinary manufacturing processes. The second method offers more possibilities. A metal with a higher resistivity than the steel used will give better results. A non metallic material, such as a plastic would probably give optimum performance, but its use would have to be weighed against other disadvantages such as less strength or fabrication difficulties.

It must be remembered that the machine used for study was never intended for use as an enclosed stator motor, and

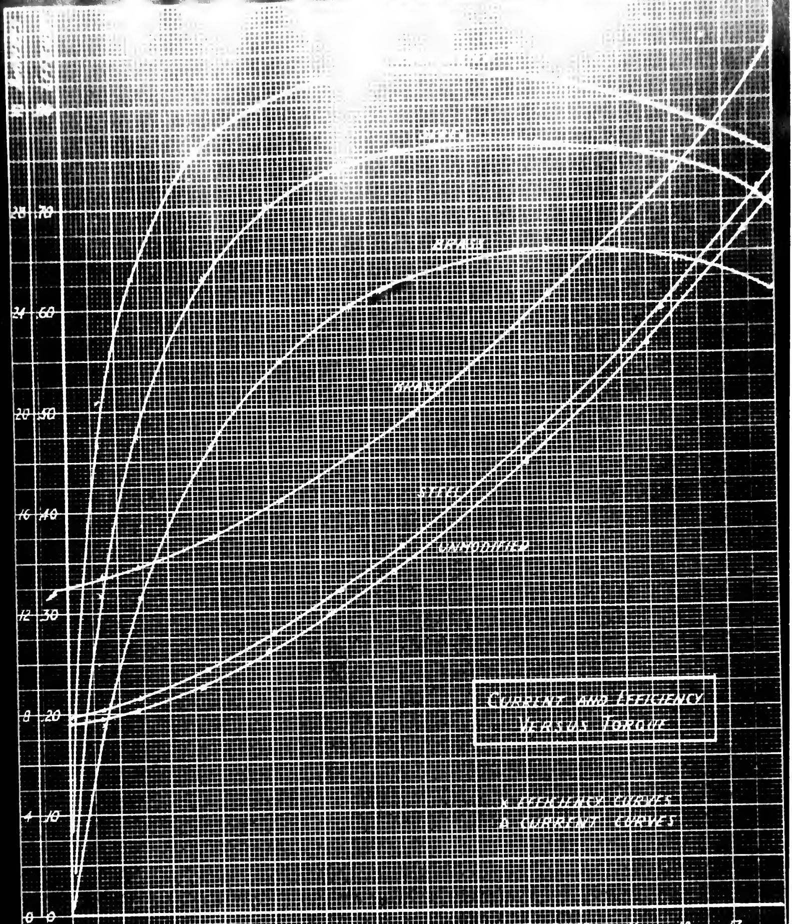
CURRENT AND EFFICIENCY
VERSUS TORQUE
X EFFICIENCY CURVES
A CURRENT CURVES
BRASS
STEEL
UNMODIFIED
TORQUE IN POUNDS FEET
0
1
2
3
4
5
6
7
8
9
10
11
12
13
0 0
4 10
8 20
12 30
16 40
20 50
24 60
28 70

FIGURE 15.

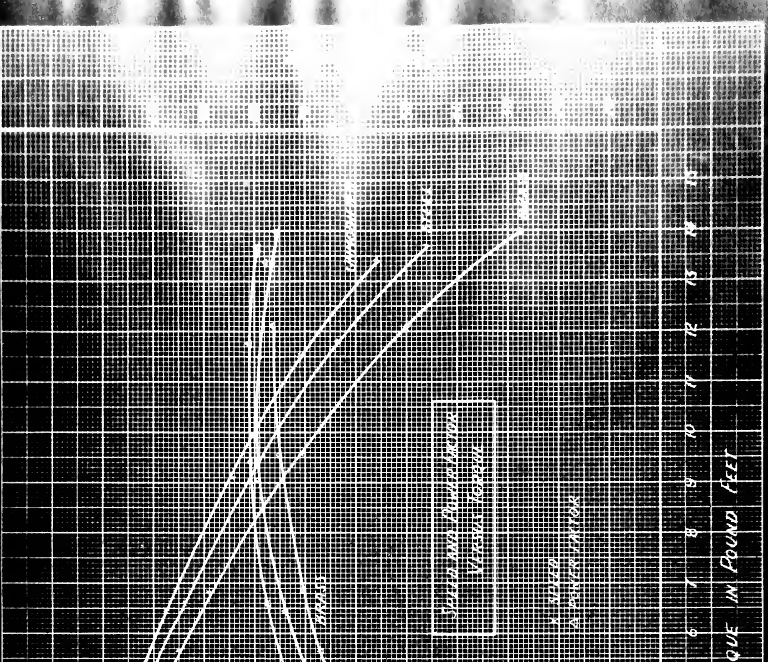
Speed and Power Factor
Versus Torque
Torque in Pound Feet
RPM
Steel
Brass
Unmodified
x Speed
Δ Power Factor

Figure 16.

consequently its performance is certainly not the maximum that could be expected from a motor specifically designed for this purpose. The author believes that the results show that a sealed stator motor is practicable and could be made to approach the performance of an ordinary type motor.

BIBLIOGRAPHY

1. Bryant and Johnson. Alternating Current Machinery.
2. Gray. Electrical Machine Design.
3. Kuhlman. Design of Electrical Apparatus. 2nd Edition
4. Lawrence. Principles of Alternating Current Machinery
5. Liwschitz, Garik and Whipple. Electrical Machinery
6. Tarboux. Alternating Current Machinery.

APPENDIX I

Name Plate Data:

5 KVA

220/110 volts

26/13 amperes

.9 p.f.

3 phase

60 cycle

1200 rpm

4.7 amps

Serial No. 4864607

2

Volts 1	Volts 2	Volts 3	Volts Av	Amps 1	Amps 2	Amps 3	Amps Av	Watts 1	Watts 2	Watts Total	VA	p f	Spd	I^2R	
268	264	262	264.7	10.5	10.1	8.6	9.73	1520	976	544	4290	.127	1196	119	Running Light
251	248	249	249.3	9.1	9.0	8.75	8.95	1320	880	440	3860	.114	1196	101	"Uncoupled"
237	234	237	236	8.3	8.4	8.2	8.3	1148	740	408	3390	.121	1196	86.7	
215	216	213	214.7	8.0	6.3	7.7	7.33	1152	760	392	2730	.143	1196	67.7	
181	180	174	178.3	7.9	6.9	3.5	6.1	664	320	344	1884	.182	1196	46.8	
166.5	158	160	161.5	6.4	5.8	4.1	5.43	588	268	320	1520	.210	1194	37.2	
144	140	142	142	4.85	5.0	4.15	4.67	428	152	276	1150	.240	1191	27.4	
128.5	126.5	127.5	127.5	4.5	4.7	3.5	4.23	384	120	264	932	.283	1190	22.6	
114	116	114.5	114.8	4.0	3.5	4.2	3.9	380	110	270	775	.348	1190	19.2	
101	102	100.5	101.2	3.8	3.1	3.65	3.52	330	85	245	616	.397	1188	15.6	
86.5	87	86.5	86.7	3.45	2.85	3.25	3.18	262	32	230	477	.482	1185	12.7	
76	77	76	76.3	3.3	2.6	3.15	3.0	238	11	227	396	.574	1180	11.3	
66	66	65	65.7	3.3	2.55	2.85	2.9	210	5	215	330	.653	1170	10.6	
55	54.5	54	54.5	3.35	2.7	2.9	2.98	180	30	210	281	.748	1155	11.2	
42	39.5	40	40.5	3.9	3.65	3.25	3.6	162	48	210	253	.830	1114	16.3	

Volts 1	Volts 2	Volts 3	Volts Av	Amps 1	Amps 2	Amps 3	Amps Av	Watts 1	Watts 2	Watts 3	Total	VA	P.F.	
92	92	94	92.7	26	23	24.5	24.5	520	410	520	1450	3930	.369	Blocked
74	74	73	73.7	20.6	17.5	19	19.0	330	200	300	830	2430	.341	
58	58	60	58.7	16	14	15.4	15.1	200	110	170	480	1532	.313	
49	51	50.5	50.2	13.7	12.1	12.1	12.6	150	80	120	350	1095	.283	
42.5	45	43	43.5	12.0	10.3	10.5	10.9	128	80	124	332	820	.397	
32.5	33.5	32	32.7	9.0	7.8	7.7	8.2	73	48	68	189	464	.401	
21.4	21.6	22.4	21.8	5.8	5.1	5.2	5.37	30	22	30	82	203	.407	
16.4	17.4	16.1	16.6	4.55	3.95	4.0	4.17	19	13	18	50	120	.404	
12.0	12.1	11.9	12.0	3.3	3.0	2.9	3.07	9.5	8	9.5	27	63.7	.427	
8.0	7.5	7.0	7.5	2.32	2.2	1.9	2.14	4.5	4.5	4.0	13	27.8	.468	

APPENDIX 2

2

	Volts				Amps				Watts							
	1	2	3	Av	1	2	3	Av	1	2	Total	VA	p f	Spd	I^2R	
	266	269	268	268	10.0	9.7	11.2	10.3	1900	800	1100	4470	.231	1198	133.7	Running Light
	258	262	260	260	9.3	9.3	10.4	9.67	1680	712	968	4350	.222	1198	117.5	with
	232	236	234	234	8.0	7.8	8.7	8.17	1360	528	832	3310	.251	1198	84.0	Steel Gr[illegible]
	206	206	214	208.7	8.2	6.0	8.4	7.53	1380	648	732	2720	.269	1198	71.5	
	186	182	198	188.7	8.5	5.4	7.2	7.03	1336	672	664	2300	.289	1198	65.3	
	160	159	166	161.7	6.2	5.1	6.2	5.83	852	340	512	1630	.314	1198	42.8	
	140	141	141	140.7	4.7	4.5	5.1	4.77	552	112	440	1160	.379	1198	28.6	
	120	127	126	124.3	3.9	3.7	5.3	4.3	460	68	392	925	.423	1195	23.3	
	102	103	106	103.7	4.2	4.2	4.2	4.2	410	40	370	753	.492	1190	22.2	
	86	84.5	89.5	86.7	4.1	3.5	3.6	3.73	342	13	329	560	.588	1185	17.5	
	73.5	73.5	75.0	74.0	3.2	3.5	3.4	3.47	255	37	292	445	.657	1175	15.2	
	61.0	62.5	62.0	61.8	3.5	3.5	3.5	3.4	204	70	274	374	.734	1165	14.6	
	51.5	51.0	53.0	51.8	3.7	3.5	3.6	3.6	196	65	261	323	.808	1138	14.3	

	Volts				Amps				Watts					
	1	2	3	Av	1	2	3	Av	1	2	Total	VA	p.f	Blocked R[illegible]
	91	91	92	91.3	22	25	24.5	23.7	80	1810	1730	3750	.462	
	72	74	74.5	72.8	17.4	19.8	20.0	19.0	60	1160	1100	2390	.461	
	57.5	58	57.5	57.7	13.9	15.7	15.0	14.9	40	660	620	1488	.418	
	52.5	53	52.5	52.7	12.6	14.1	13.7	13.5	40	540	500	1232	.406	
	44	44.3	43.5	43.9	10.3	11.1	11.7	11.0	20	390	370	835	.443	
	33	34	32.3	33.1	7.6	8.4	8.9	8.3	15	228	213	476	.447	
	24.2	23.5	23.2	23.6	5.5	5.7	6.3	5.84	5	112	107	239	.447	
	17.7	16.8	16.7	17.1	4.15	3.95	4.5	4.2	0	53	53	124	.428	
	10.5	8.0	9.0	9.2	2.65	2.1	2.6	2.45	4	15	19	39	.487	

Appendix 3

	Volts				Amps				Watts							
	1	2	3	Av	1	2	3	Av	1	2	Total	VA	pf	Spd	I^2R	
	236	233	231	233.3	13.8	14.0	14.3	14.03	3080	1280	1800	5670	.318	1190	248	Ru[illegible] L[illegible]
	205	200	200	201.7	13.0	13.0	13.2	13.07	2520	1200	1320	4560	290	1190	215	with
	202	197	197	198.7	11.6	11.6	11.7	11.63	2190	900	1290	4030	320	1190	170.5	Brass Cr[illegible]
	195	189	190	191.3	11.1	10.7	11.2	11.0	2014	800	1214	3680	330	1190	152	
	183.5	178.5	180	180.7	10.4	10.2	10.5	10.37	1760	700	1000	3246	.309	1190	135.2	
	163.5	158.5	160.5	160.8	9.4	9.3	9.4	9.37	1386	580	806	2610	.309	1190	110.5	
	118	117	118	117.7	7.65	7.65	7.65	7.65	924	424	500	1550	.322	1184	73.7	
	89	89.2	89.5	89.3	5.9	6.1	6.0	6.0	534	130	404	928	.436	1178	45.3	
	84	80	83	82.3	5.8	5.9	6.0	5.9	480	100	380	840	.452	1170	43.8	
	70.5	70.2	70.5	70.4	5.1	5.1	5.25	5.15	338	20	358	628	.570	1164	33.4	
	56.5	56.5	57.0	56.7	4.9	4.9	4.75	4.85	255	95	340	467	.729	1158	29.6	
	44.5	44.5	44.0	44.3	4.9	4.9	4.9	4.9	194	132	326	376	.867	1100	30.2	
	39.2	38.5	40.0	39.2	5.15	5.1	5.2	5.15	195	106	301	350	.860	1050	33.4	
	32.4	33.0	32.3	32.5	6.2	6.3	6.4	6.2	195	85	270	354	.760	955	50.0	

	Volts				Amps				Watts						
	1	2	3	Av	1	2	3	Av	1	2	3	Total	VA	P.F.	Blocked Rot[illegible]
	96	95	94	95	27.5	28.5	27.5	27.8	800	800	864	2464	4570	.539	
	74	68	70	70.7	20.5	21.3	19.5	20.4	435	440	420	1295	2490	.52	
	58	56.5	55	56.5	16.9	17.0	16.3	16.73	245	230	290	765	1635	.468	
	54	51	50	51.7	14.9	14.3	15.0	14.73	190	160	266	616	1320	.467	
	48	49.5	48.5	48.7	14.4	14.2	13.6	14.07	167	140	216	523	1185	.441	
	42.5	41.0	42.2	41.9	11.8	12.4	11.8	12.0	154	168	160	422	867	.487	
	32.4	30.8	31.7	31.63	8.8	9.3	8.7	8.93	90	94	90	274	490	.558	
	15	15.2	16.7	15.63	4.15	4.58	4.62	4.45	18	21	25	64	120.5	542	
	7	7	8	7.33	2.0	2.5	2.6	2.37	5	5	7	17	30.1	.565	

Appendix 4

APPENDIX V

CIRCUIT PARAMETERS, AND CIRCLE DIAGRAM VALUES

	Unmodified	Steel	Brass
I_b	13	13	13
P_o	415	468-43	485-50
V_b	52	50.5	46
$I = \frac{V}{V_b} I_b$	54.9	56.5	62.0
$Z_o = V_b / I_b \sqrt{3}$	2.31	2.25	2.05
$R_o = P_b / 3 I_b^2$	.82	.906	.95
R_1 (Corrected)	.398	.422	.43
R_2	.422	.484	.52
$X_o = \sqrt{Z_o^2 - R_o^2}$	2.16	2.06	1.82
$X_1 = X_2 = X_o / 2$	1.08	1.03	.91
P NO LOAD	390	763	1595
I_o	7.6	7.8	13
$I_l = P / V\sqrt{3}$	1.02	2.0	4.19
$I_m = \sqrt{I_o^2 - I_l^2}$	7.54	7.54	12.3
$g_e = I_l \sqrt{3} / V$	.00798	.0157	.0328
$b_e = I_m \sqrt{3} / V$	.0594	.0594	.0966
$MO = I_o$	7.6	7.8	13.0
$MN = I_l$	1.02	2.0	4.19
$MB = I$	54.9	56.5	62.0
$BF = \frac{R_o}{Z_o} MB$	19.5	22.8	28.7
$P = (\overline{MB}^2 - \overline{MO}^2) R_1$	1180	1320	1580
$EG = P\sqrt{3} / V$	9.3	10.4	12.4
$MF = \sqrt{\overline{MB}^2 - \overline{BF}^2}$	51.3	51.6	55.0
$NO = \sqrt{\overline{MO}^2 - \overline{MN}^2}$	7.54	7.54	12.3
$OE = MF - NO$	43.76	44.06	42.7

	Unmodified	Steel	Brass
$BE = BF - MN$	18.48	20.8	24.51
$OB = \sqrt{\overline{BE}^2 + \overline{OE}^2}$	47.5	48.8	49.2
$OA = \dfrac{\overline{OB}^2}{OE}$	52.0	54.0	56.7

DATA FROM CIRCLE DIAGRAMS

θ_{25}	OD	KD	LD	PD	PK	PL	PC	I_1	RPM	EFFIC	PF	TORQUE	
0	0	0	0	0	0	0	1.02	7.6	1200	0	134	0	UNMODIFIED
1	.0156	00332	00657	905	.9017	.898	1.925	7.8	1196	.466	.248	67	
2	0631	0135	0266	1.81	1.797	1.783	2.83	8.1	1190	.63	.35	134	
4	.251	.0535	106	3.62	3.57	3.514	4.64	9.05	1183	.758	.512	2.66	
6	.57	1215	.24	5.4	5.278	5.16	6.42	10.35	1173	798	.62	3.93	
8	1.01	215	.425	7.22	7.0	6.795	8.24	11.9	1164	.824	.693	5.2	
10	1.57	.335	.661	8.9	8.56	8.24	9.92	13.45	1155	.832	.738	6.45	
15	3.47	.74	1.465	13	12.26	11.53	14.02	17.8	1129	.826	.788	9.1	
20	6.08	1.295	2.56	16.7	15.4	14.14	17.72	22.4	1102	.798	.79	11.5	
25	9.25	1.97	3.9	19.9	17.93	16.0	20.92	26.8	1071	.756	.78	13.4	
0	0	0	0	0	0	0	2.0	7.8	1200	0	.256	0	WITH STEEL
1	.0162	00382	00765	.94	.9362	.9324	2.94	8.12	1195	.317	.362	.7	
2	.0655	.01545	0309	1.88	1.865	1.849	3.88	8.55	1190	.476	.454	1.39	
4	.261	.0615	.123	3.75	3.69	3.63	5.75	9.7	1181	.632	.593	2.75	
6	.59	.139	.278	5.6	5.46	5.32	7.6	11.1	1169	.70	.685	4.07	
8	1.045	.247	493	7.5	7.25	7.0	9.5	12.8	1159	.735	.742	5.4	
10	1.63	.384	.77	9.25	8.87	8.48	11.25	14.5	1147	.754	.776	6.6	
15	3.6	.85	1.7	13.5	12.65	11.8	15.5	19.1	1119	.761	.812	9.4	
20	6.31	1.49	2.98	17.35	15.86	14.37	19.35	23.8	1087	.744	.813	11.8	
25	9.6	2.26	4.53	20.6	18.34	16.07	22.6	28.4	1052	.71	.795	13.7	
0	0	0	0	0	0	0	4.19	13	1200	0	.322	0	WITH BRASS
1	.017	.00493	.00975	985	.98	.9753	5.175	13.5	1194	.188	.383	.73	
2	.069	.02	.0396	1.97	1.95	1.93	6.16	13.8	1188	313	447	1.45	
4	.274	.0795	157	3.94	3.86	3.78	8.13	15.0	1175	.465	543	2.88	
6	.62	18	.356	5.9	5.72	5.54	10.1	16.4	1162	548	616	4.26	
8	1.1	.319	.63	7.85	7.53	7.22	12.05	18.1	1151	.60	.67	5.65	
10	1.71	495	.98	9.72	9.22	8.74	13.9	19.7	1138	.629	.705	6.86	
15	3.78	1.095	2.17	14.15	13.05	11.98	18.34	24.4	1102	654	752	9.55	
20	6.63	1.92	3.8	18.2	16.3	14.4	22.4	29.3	1060	.643	.765	12.1	APPENDIX 6
25	10.1	2.93	5.8	21.6	18.7	15.8	25.8	34.3	1015	.613	.755	14.0	

87

Thesis 15559
R243 Rathbun
An investigation of
the performance of an
induction type motor with
metal inclosed stator.